

Supporting Information

Theoretical prediction of 2D biphenylene as a potential anchoring material for lithium-sulfur batteries

Han Wang, Fan Kong, Zonggang Qiu, Jiyuan Guo*, Huabing Shu, Qin Wei
School of Science, Jiangsu University of Science and Technology, Zhenjiang, 212100, China

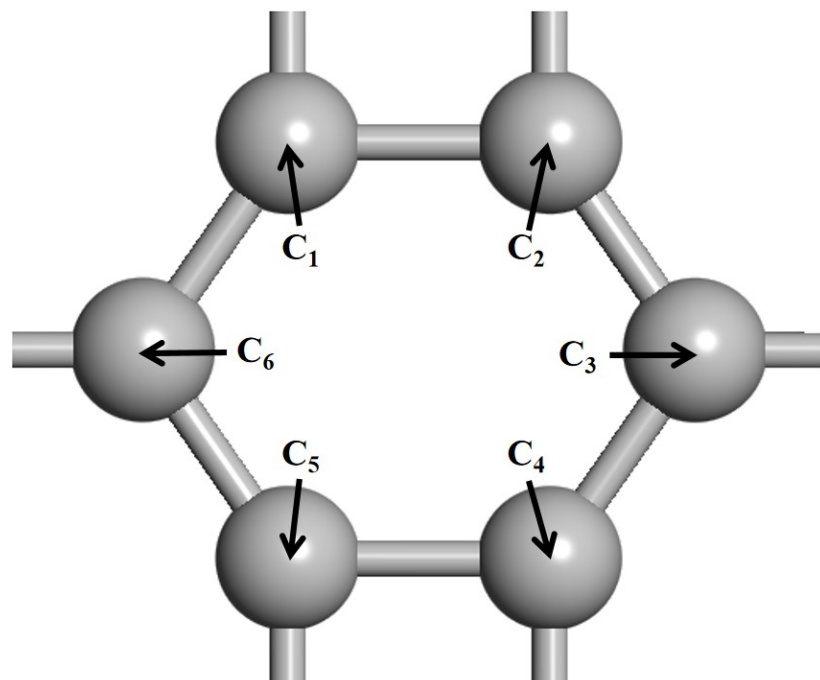


Fig. S1 The schematic diagram of the unit cell of 2D biphenylene (BIP).

Table S1 The calculated adsorption energies (E_{ads}), the average adsorption heights (H_{ave}), Li-S bond lengths (D_{Li-S}) and S-S bond lengths (D_{S-S}) of LiPSs adsorbed on the BIP.

Cluster	S_8	Li_2S_8	Li_2S_6	Li_2S_4	Li_2S_2	Li_2S
$H_{ave}(\text{\AA})$	3.08	1.99	1.98	2.20	1.80	1.50
$E_{ads}(\text{eV})$	1.05	1.59	1.37	1.25	2.16	2.55
$D_{Li-S}(\text{\AA})$	/	2.39	2.41	2.37	2.23	2.06
$D_{S-S}(\text{\AA})$	2.08	2.01	2.05	2.11	2.22	/

*Corresponding author
E-mail address: jyguo@just.edu.cn

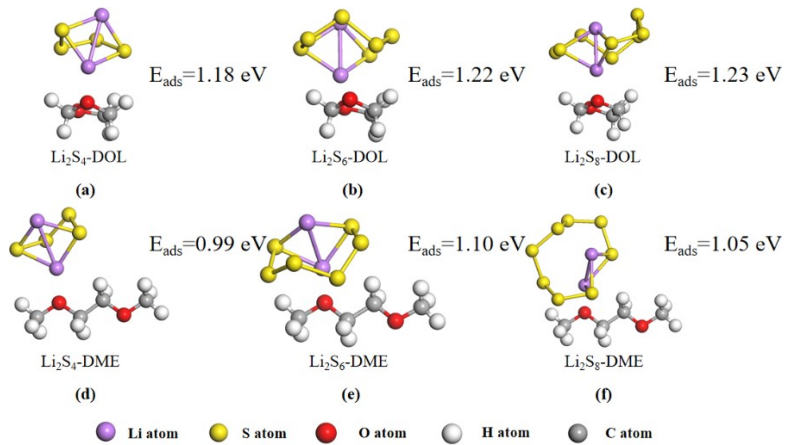


Fig. S2 Optimized structures and adsorption energies between Li_2S_n ($n = 4, 6, 8$) and DME/DOL.

Table S2 The calculated adsorption energies of Li_2S_n ($n = 8, 6, 4$) with the electrolyte solvents DOL and DME.

Cluster	Li_2S_8	Li_2S_6	Li_2S_4
$E_{\text{ads}}\text{-DOL (eV)}$	1.23	1.22	1.18
$E_{\text{ads}}\text{-DME (eV)}$	1.05	1.10	0.99

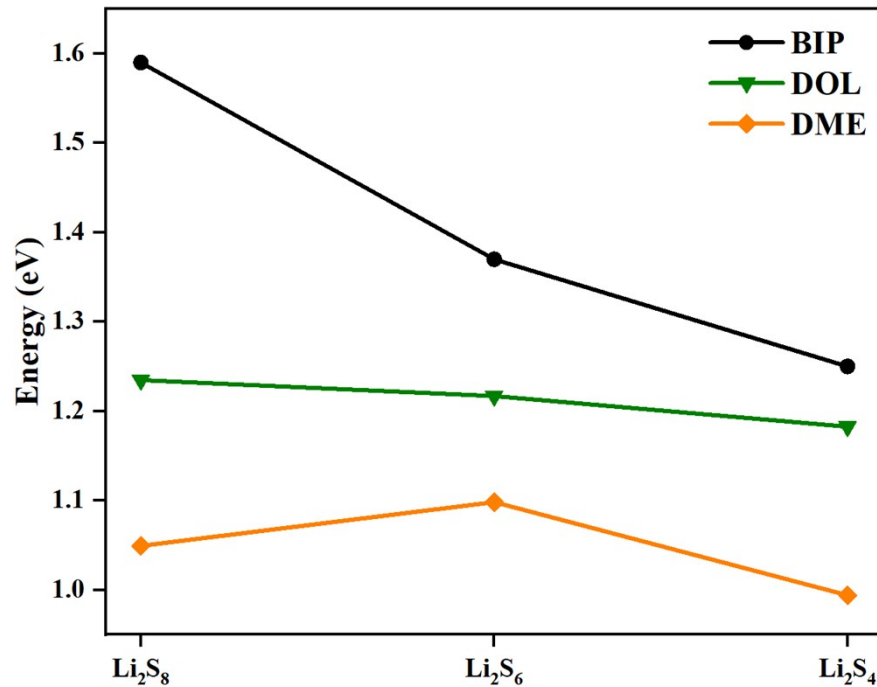


Fig. S3 Adsorption energy of Li_2S_n ($n = 8, 6, 4$) on BIP and interaction energy of LiPSs with DME and DOL.

Table S3 The formation energies of the M (M = B, N, O, F, Br) atoms doped BIP

Element	B	N	O	F	Br
E_f-T_1 (eV)	-0.77	-1.28	9.69	0.91	3.80
E_f-T_2 (eV)	-0.55	-0.75	11.44	2.31	4.07

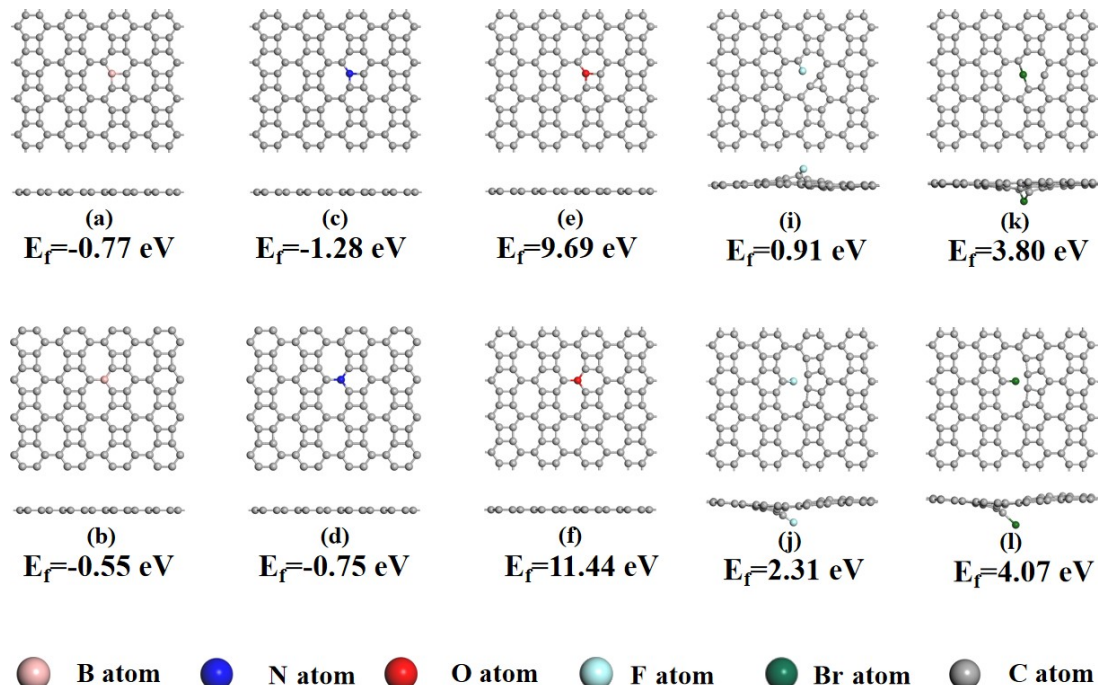


Fig. S4 Optimized structures of doped M atoms (M = B, N, O, F, Br), a-l corresponding the optimized structures of B, N, O, F, Br atom replacing C atom at T_1/T_2 site, respectively.

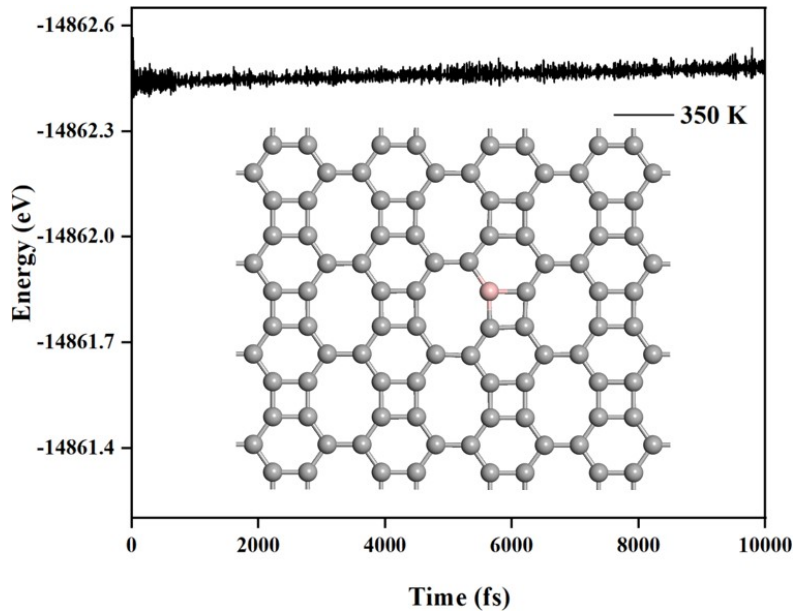


Fig. S5 Top views of the optimized B doped BIP structures and AIMD simulations results at 350 K lasting for 10 ps of the B doped BIP monolayer.

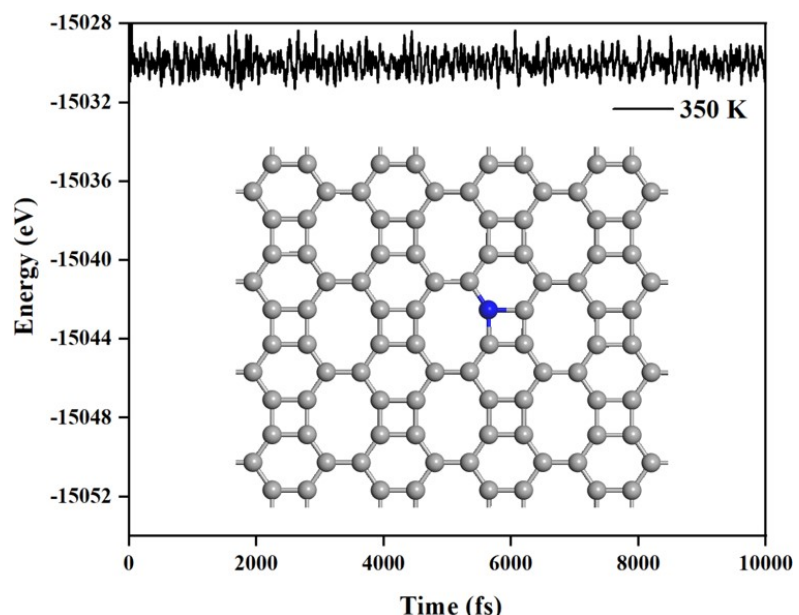


Fig. S6 Top views of the optimized N doped BIP structures and AIMD simulations results at 350 K lasting for 10 ps of the N doped BIP monolayer.

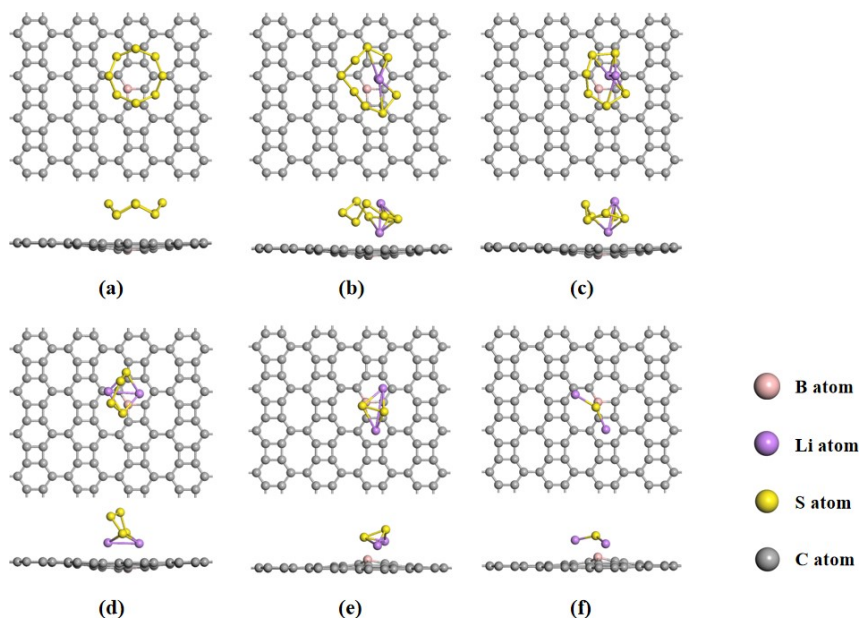


Fig. S7 Top and side views of the most stable adsorption configurations for (a) S_8 @BIP and (b)-(f) Li_2S_n ($n = 8, 6, 4, 2, 1$)@B doped BIP.

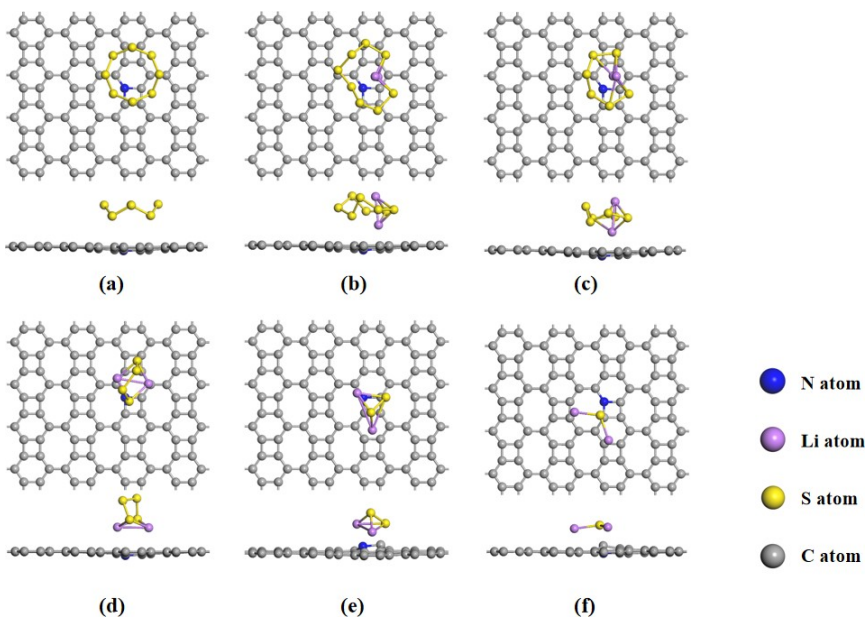


Fig. S8 Top and side views of the most stable adsorption configurations for (a) S_8 @BIP and (b)-(f) Li_2S_n ($n = 8, 6, 4, 2, 1$)@N doped BIP.

Table S4 The calculated adsorption energies (E_{ads}), the average adsorption heights (H_{ave}), Li-S bond lengths(D_{Li-S}) and S-S bond lengths(D_{S-S}) of LiPSs adsorbed on the B doped BIP.

Cluster	S ₈	Li ₂ S ₈	Li ₂ S ₆	Li ₂ S ₄	Li ₂ S ₂	Li ₂ S
H _{ave} (Å)	3.12	1.98	1.97	2.17	1.26	1.09
E _{ads} (eV)	1.06	1.67	1.46	1.38	2.38	2.86
D _{Li-S} (Å)	/	2.49	2.46	2.47	2.43	2.27
D _{S-S} (Å)	2.09	2.10	2.11	2.10	2.13	/

Table S5 The calculated adsorption energies (E_{ads}), the average adsorption heights (H_{ave}), Li-S bond lengths(D_{Li-S}) and S-S bond lengths(D_{S-S}) of LiPSs adsorbed on the N doped BIP.

Cluster	S ₈	Li ₂ S ₈	Li ₂ S ₆	Li ₂ S ₄	Li ₂ S ₂	Li ₂ S
H _{ave} (Å)	3.12	2.13	2.04	2.37	1.36	1.13
E _{ads} (eV)	1.03	1.38	1.22	1.05	2.14	2.75
D _{Li-S} (Å)	/	2.46	2.43	2.41	2.39	2.25
D _{S-S} (Å)	2.09	2.11	2.11	2.10	2.14	/

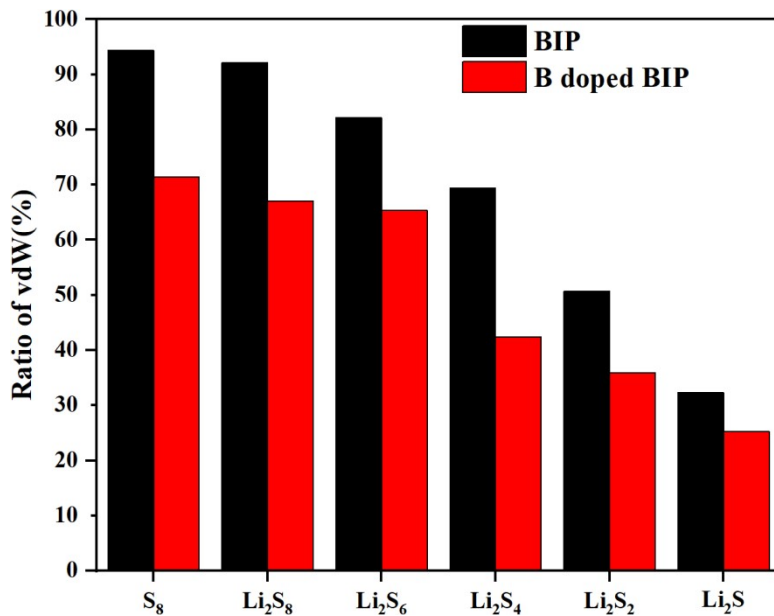


Fig. S9 (a) Proportion of vdW interactions between the intrinsic and B doped BIP at different stages of lithiation.

Gibbs free energy calculation of sulfur reduction reaction (SRR) in vacuum and BIP Surface

Overall, the SRR during the discharge of Li-S batteries is a 16 electrons process with the formation of eight Li₂S molecules



The rudimentary step involved in the generation of one Li_2S molecules is as follows;



Wherein * represents an active site on the catalytic substrate

The Gibbs free energy (ΔG) for each SRR during the Li-S discharge process is calculated as

$$\Delta G = \Delta E + \Delta E_{ZPE} - T\Delta S \quad (S7)$$

Where ΔE represents the adsorption energy and ΔE_{ZPE} and $T\Delta S$ denotes the zero point energy difference and entropy difference between the gas phase and adsorbed phase calculated from the frequency calculations at 298.15 K.

The change in Gibbs free energy for each SRR electrochemical steps is attained from the given relations;

$$\begin{aligned} \Delta G_1 = & (E_{*Li_2S_8} + E_{ZPE(*Li_2S_8)} - TS_{*Li_2S_8}) - (E_{*S_8} + E_{ZPE(*S_8)} - TS_{*S_8}) \\ & - 2(E_{Li} + E_{ZPE(Li)} - TS_{Li}) \end{aligned} \quad (S8)$$

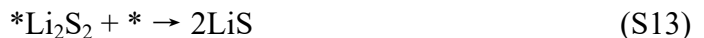
$$\begin{aligned} \Delta G_2 = & (E_{*Li_2S_6} + E_{ZPE(*Li_2S_6)} - TS_{*Li_2S_6}) + 1/4(E_{*S_8} + E_{ZPE(*S_8)} - TS_{*S_8}) \\ & - (E_{*Li_2S_8} + E_{ZPE(*Li_2S_8)} - TS_{*Li_2S_8}) \end{aligned} \quad (S9)$$

$$\begin{aligned} \Delta G_3 = & (E_{*Li_2S_4} + E_{ZPE(*Li_2S_4)} - TS_{*Li_2S_4}) + 1/4(E_{*S_8} + E_{ZPE(*S_8)} - TS_{*S_8}) \\ & - (E_{*Li_2S_6} + E_{ZPE(*Li_2S_6)} - TS_{*Li_2S_6}) \end{aligned} \quad (S10)$$

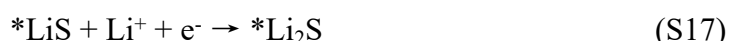
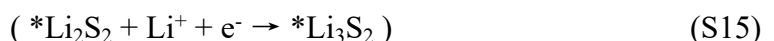
$$\begin{aligned} \Delta G_4 = & (E_{*Li_2S_2} + E_{ZPE(*Li_2S_2)} - TS_{*Li_2S_2}) + 1/4(E_{*S_8} + E_{ZPE(*S_8)} - TS_{*S_8}) \\ & - (E_{*Li_2S_4} + E_{ZPE(*Li_2S_4)} - TS_{*Li_2S_4}) \end{aligned} \quad (S11)$$

$$\begin{aligned} \Delta G_5 = & (E_{*Li_2S} + E_{ZPE(*Li_2S)} - TS_{*Li_2S}) + 1/8(E_{*S_8} + E_{ZPE(*S_8)} - TS_{*S_8}) \\ & - (E_{*Li_2S_2} + E_{ZPE(*Li_2S_2)} - TS_{*Li_2S_2}) \end{aligned} \quad (S12)$$

Pathway a:



Pathway b:



Pathway c:



Wherein * represents an active site on the catalytic substrate.

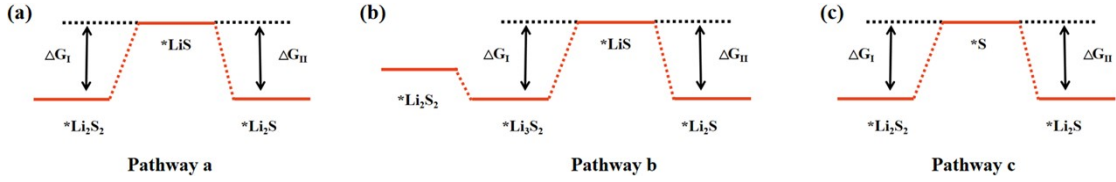


Fig. S10 The Gibbs energy differences for the first step (ΔG_I) and the second step (ΔG_{II}) of three possible reaction pathways in the conversion from Li_2S_2 to Li_2S .

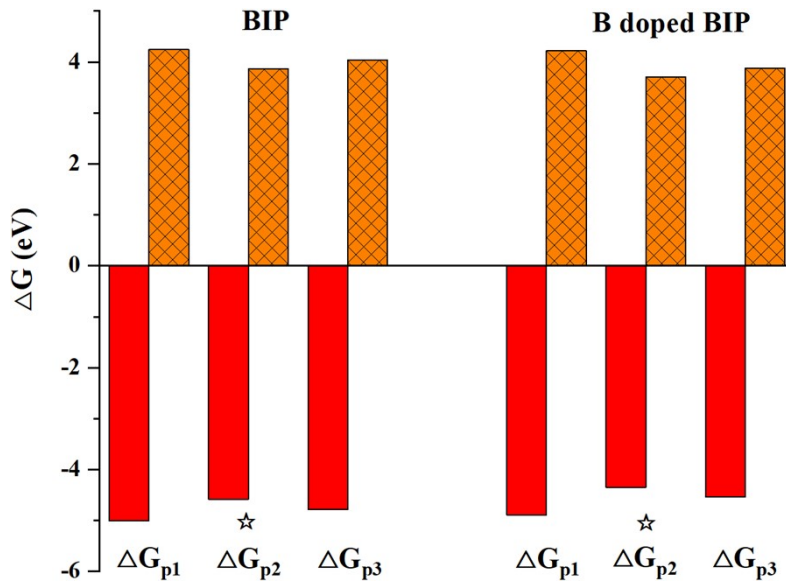


Fig. S11 The Gibbs energy differences for two elementary steps in every possible pathway. The pentagram symbols indicate the optimal reaction pathway on intrinsic and B doped BIP. Yellow with gridding, and red without gridding represent the Gibbs energy differences for the first step (ΔG_I) and the second step (ΔG_{II}), respectively.

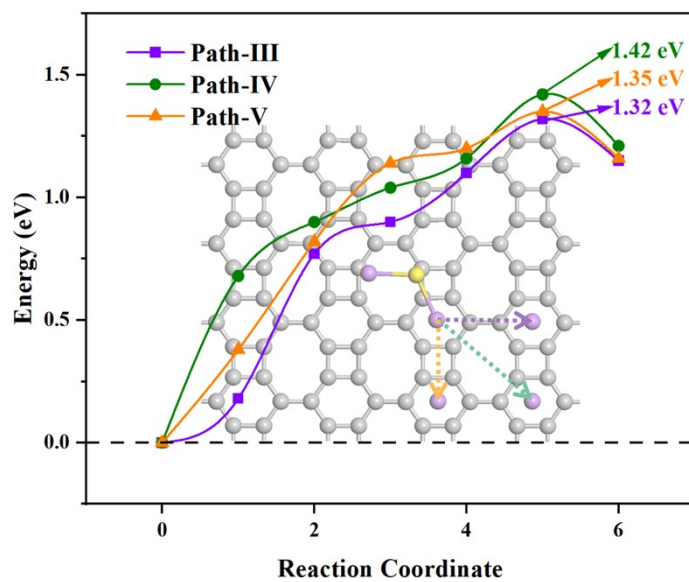


Fig. S12 Paths of Li_2S decomposition and the corresponding energy barriers on the BIP